



# **Interpupillary and Vertex Distance Effects on Field-of-View and Acuity with ANVIS**

**By**

**James M. King**

**and**

**Stephen E. Morse**

**Sensory Research Division**

**January 1992**

**93-03665**



**Approved for public release; distribution unlimited.**

**United States Army Aeromedical Research Laboratory  
Fort Rucker, Alabama 36362-5292**

## Notice

### Qualified requesters

Qualified requesters may obtain copies from the Defense Technical Information Center (DTIC), Cameron Station, Alexandria, Virginia 22314. Orders will be expedited if placed through the librarian or other person designated to request documents from DTIC.

### Change of address

Organizations receiving reports from the U.S. Army Aeromedical Research Laboratory on automatic mailing lists should confirm correct address when corresponding about laboratory reports.

### Disposition

Destroy this report when it is no longer needed. Do not return to the originator.


### Disclaimer

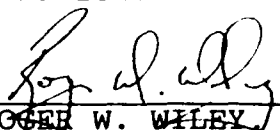
The views, opinions, and/or findings contained in this report are those of the authors and should not be construed as an official Department of the Army position, policy, or decision, unless so designated by other official documentation. Citation of trade names in this report does not constitute an official Department of the Army endorsement or approval of the use of such commercial items.

### Human use

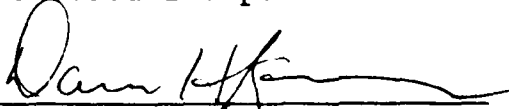
Human subjects participated in these studies after giving their free and informed voluntary consent. Investigators adhered to AR 70-25 and USAMRDC Reg 70-25 on Use of Volunteers in Research.

### Reviewed:

  
RICHARD R. LEVINE  
LTC, MS  
Director, Sensory Research  
Division

  
ROGER W. WILEY, O.D., Ph.D.  
Chairman, Scientific  
Review Committee

### Released for publication:

  
DAVID H. KARNEY  
Colonel, MC, SFS  
Commanding

REPORT DOCUMENTATION PAGE				Form Approved OMB No. 0704-0188	
1a. REPORT SECURITY CLASSIFICATION <b>Unclassified</b>			1b. RESTRICTIVE MARKINGS		
2a. SECURITY CLASSIFICATION AUTHORITY			3. DISTRIBUTION / AVAILABILITY OF REPORT <b>Approved for public release; distribution unlimited</b>		
2b. DECLASSIFICATION / DOWNGRADING SCHEDULE					
4. PERFORMING ORGANIZATION REPORT NUMBER(S) <b>USAARL Report No. 93-9</b>			5. MONITORING ORGANIZATION REPORT NUMBER(S)		
6a. NAME OF PERFORMING ORGANIZATION <b>U.S. Army Aeromedical Research Laboratory</b>		6b. OFFICE SYMBOL (If applicable) <b>SGRD-UAS-VS</b>	7a. NAME OF MONITORING ORGANIZATION <b>U.S. Army Medical Research and Development Command</b>		
6c. ADDRESS (City, State, and ZIP Code) <b>P.O. Box 577 Fort Rucker, AL 36362-5292</b>			7b. ADDRESS (City, State, and ZIP Code) <b>Fort Detrick Frederick, MD 21702-5012</b>		
8a. NAME OF FUNDING / SPONSORING ORGANIZATION		8b. OFFICE SYMBOL (If applicable)	9. PROCUREMENT INSTRUMENT IDENTIFICATION NUMBER		
8c. ADDRESS (City, State, and ZIP Code)			10. SOURCE OF FUNDING NUMBERS		
			PROGRAM ELEMENT NO <b>0602787A</b>	PROJECT NO <b>3M1627 87A879</b>	TASK NO. <b>BG</b>
11. TITLE (Include Security Classification) <b>(U) Interpupillary and Vertex Distance Effects on Field-of-View and Acuity with ANVIS</b>					
12. PERSONAL AUTHOR(S) <b>King, James M., and Morse, Stephen E.</b>					
13a. TYPE OF REPORT <b>Final</b>		13b. TIME COVERED FROM _____ TO _____		14. DATE OF REPORT (Year, Month, Day) <b>1993 January</b>	
15. PAGE COUNT <b>35</b>					
16. SUPPLEMENTARY NOTATION					
17. COSATI CODES			18. SUBJECT TERMS (Continue on reverse if necessary and identify by block number) <b>Field-of-View, acuity, ANVIS, night vision</b>		
FIELD	GROUP	SUB-GROUP			
<b>23</b>	<b>02</b>				
19. ABSTRACT (Continue on reverse if necessary and identify by block number) <b>Third generation Aviation Night Vision Imaging Systems (ANVIS) employ vertical, tilt, interpupillary distance, vertex distance, and focus adjustments. ANVIS field-of-view is nominally 40 degrees but can be limited by adjustments. Interpupillary distance effects on ANVIS field-of-view have been computed, but seldom measured. There have been reports of acuity loss at the periphery of ANVIS fields-of-view. Fields-of-view were measured in 10 subjects, acuities in 8. ANVIS were used with a 10-foot working distance. Acuities were assessed using Bailey-Lovie charts. At the 18 mm vertex distance, binocular and monocular fields-of-view decreased with decentration. At the 32 mm vertex distance, binocular and monocular fields-of-view were reduced at optimal interpupillary distance, and decreased with increasing decentration. The total horizontal field-of-view at 32 mm vertex distance was increased by increasing decentration, offsetting the reduction caused by increased vertex distance. Acuity was relatively insensitive to changes in vertex distance and interpupillary distance, but was substantially reduced in the periphery of the field-of-view, and under low contrast.</b>					
20. DISTRIBUTION / AVAILABILITY OF ABSTRACT <input checked="" type="checkbox"/> UNCLASSIFIED / UNLIMITED <input type="checkbox"/> SAME AS RPT <input type="checkbox"/> DTIC USERS			21. ABSTRACT SECURITY CLASSIFICATION <b>Unclassified</b>		
22a. NAME OF RESPONSIBLE INDIVIDUAL <b>Chief, Scientific Information Center</b>			22b. TELEPHONE (Include Area Code) <b>(205) 255-6907</b>		22c. OFFICE SYMBOL <b>SGRD-UAX-SI</b>

## Table of contents

List of figures.....	2
List of tables.....	4
Introduction.....	5
Methods.....	9
Subjects.....	9
ANVIS.....	9
Field-of-view.....	11
Acuity.....	12
Experimental sequence.....	13
Results.....	13
Discussion.....	22
Field-of-view.....	22
Acuity.....	25
Conclusions.....	28
References.....	29
Appendixes	
Appendix A - List of equipment manufacturers.....	32
Appendix B - Data collection forms.....	33

Accession For	
NTIS	CRA&I <input checked="" type="checkbox"/>
DTIC	TAB <input type="checkbox"/>
Unannounced <input type="checkbox"/>	
Justification .....	
By .....	
Distribution / .....	
Availability Codes	
Dist	Avail and/or Special
A-1	

### List of figures

1. Predicted components of the field-of-view at 18 mm vertex distance.....	7
2. Predicted components of the field-of-view at 32 mm vertex distance.....	7
3. Relative contributions to the field-of-view at 18 mm vertex distance.....	8
4. Relative contributions to the field-of-view at 32 mm vertex distance.....	8
5. Front view of the apparatus.....	10
6. Rear view of the apparatus.....	10
7. Average single tube field-of-view.....	15
8. 18 mm vertex distance, average single tube field-of-view..	15
9. 32 mm vertex distance, average single tube field-of-view..	15
10. Binocular field-of-view.....	16
11. 18 mm vertex distance, binocular field-of-view.....	16
12. 32 mm vertex distance, binocular field-of-view.....	16
13. Monocular lobe size.....	17
14. 18 mm vertex distance, monocular lobe size.....	17
15. 32 mm vertex distance, monocular lobe size.....	17
16. Total field-of-view.....	19
17. 18 mm vertex distance, total field-of-view.....	19
18. 32 mm vertex distance, total field-of-view.....	19
19. Acuity at 18 mm vertex distance.....	21
20. Acuity at 32 mm vertex distance.....	21
21. Acuity at 18 mm vertex distance, center of field.....	23
22. Acuity at 18 mm vertex distance, periphery of field.....	23
23. Acuity at 32 mm vertex distance, center of field.....	24

24. Acuity at 32 mm vertex distance, periphery of field.....	24
25. Observed relative contributions to the field-of-view at 18 mm vertex distance.....	26
26. Observed relative contributions to the field-of-view at 32 mm vertex distance.....	26

### List of tables

1. Conversion from logMAR to Snellen Denominators (20/-)..... 20
2. Single tubes fields-of-view in degrees as a function of  
vertex distance..... 22
3. Acuity in logMAR at the center and periphery of the  
ANVIS field of view for approximately equivalent  
lighting conditions..... 25

## Introduction

In addition to focus, several fitting adjustments must be accomplished by the individual aviator to optimize performance of Aviation Night Vision Imaging System (ANVIS, AN/AVS-6) night vision goggles. These adjustments include vertical alignment, tilt, interpupillary distance (IPD), and vertex distance (Loro, 1991; TC1-204, 1988; U.S. Army Aviation Center, 1991). The ANVIS field-of-view is usually reported to be 40 degrees, and Walsh (1989) found that the mean field-of-view for 5 sets of ANVIS was 39.8 degrees, but adjustment changes can limit an aviator's ability to obtain a full and complete 40 degree field-of-view (Loro, 1991; Verona and Rash, 1989). A restricted field-of-view reduces performance on a variety of complex tasks (Wells and Venturino, 1989). In addition, there has recently been considerable interest in the possible operational impacts of ANVIS adjustments. The specific impetus for this investigation is a tasking memorandum from Headquarters, Medical Research and Development Command relating to the potential contributions of IPD adjustments to a Class A OH-58D mishap (Parry, 1992).

Walsh (1990) reported that the ANVIS field-of-view declines from 40 degrees at 20 mm vertex distance to 27 degrees at 40 mm vertex distance. Kotulak and Frezell (1991) also demonstrated that increases in vertex distance produce systematic decreases in goggle field-of-view. Kotulak (in preparation) has found that changes in the vertex distance setting of ANVIS can have substantial effects on the available field-of-view. He reported that the as worn vertex distances ranged from 15 mm for the fifth percentile aviator to 32 mm for the 95th percentile aviator. Fields-of-view ranged from 40 degrees at vertex distances of 18 mm or less down to 32 degrees at the 32 mm vertex distance. Vertex distances greater than 18 mm restrict the field-of-view in direct proportion to the increase in vertex distance. The majority of the extended vertex distances noted by Kotulak were attributed to the lack of vertex distance adjustment range in the ANVIS, rather than to deliberate or accidental misadjustment.

Four measures of field-of-view are relevant to the present discussion. They are the single tube field-of-view, the binocular field-of-view, the monocular lobe size, and the total field-of-view. The average single tube field-of-view is the mean of the angular sizes of the two single tube fields-of-view. The binocular field-of-view is the angular area which is visible through both tubes simultaneously. The monocular lobe size is the combined angular extent of the two monocular lobes, which are areas visible through only one tube. The total field-of-view extends from the left to the right edge of the area visible through either tube, and represents the total angular area visible through one or both tubes. It consists of the binocular field-of-view plus the monocular lobe size.



Several theoretical analyses of the effects of changes in vertex distance and IPD on ANVIS fields-of-view have been conducted within the Visual Science Branch. Kotulak (1992) concluded that increased vertex distance would reduce the single tube field-of-view, and that decentration would produce vignetting on one side of the field-of-view, reducing its size. Specifically, nasal decentration would produce temporal vignetting in both single tube fields, while temporal decentration would produce nasal vignetting in both single tube fields. McLean (1992) concluded that decentration would increase the total field-of-view at 32 mm vertex distance, but not at 18 mm vertex distance, where it would remain 40 degrees regardless of the extent of decentration. This argument is presented graphically in Figures 1 and 2. McLean also predicted that, at 18 mm vertex distance, setting the ANVIS IPD to other than the optimal distance for a subject will result in reductions of the binocular field-of-view. The single tube fields-of-view will be vignetted on one edge, but when both fields are combined, the total field-of-view will be unchanged. This is shown in Figure 3. However, at a vertex distance of 32 mm, McLean expected ANVIS to deliver a reduced total field-of-view, which would be restored by decentration. This is shown in Figure 4. Thus, setting the IPD of ANVIS to other than the separation matching the observer's IPD should have the effect of transforming ANVIS into a partially overlapped system. The contribution of IPD setting changes to the size of the areas, the binocular field-of-view and the monocular lobe, making up the total field-of-view were expected to vary as a function of vertex distance.

Previous research at USAARL has also indicated that there is a small loss in resolution (0.07 logMAR) at the periphery of ANVIS fields-of-view when compared to the resolution at the center of the field-of-view (Walsh, unpublished, cited in Karney, 1988). The term logMAR refers to the log of the minimum angle of resolution. However, as this finding was never formally documented in a report, controlled measurements of acuity were included in the present experiment.

There is a small, but consistent advantage in resolution and contrast sensitivity to be derived from binocular as opposed to monocular viewing (Arditi, 1986; Boff and Lincoln, 1988). As an ANVIS with its IPD set to other than the optimal value is also a partially monocular device, changes in visual performance in the monocular portions of the field-of-view might be expected. However, Wiley (1989) found little impact of monocular viewing on acuity with AN/PVS-5A night vision devices. Previous investigators have noted strong effects of target contrast on acuity with the AN/PVS-5A (Wiley, 1989) and with ANVIS (Kotulak and Rash, 1992). Thus, lower acuity was also anticipated for low contrast targets compared to high contrast targets.

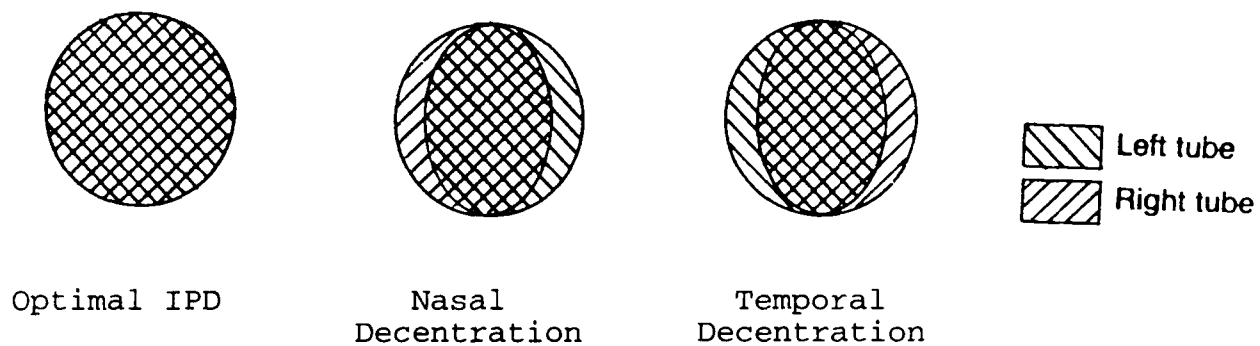


Figure 1. Predicted components of the field-of-view at 18 mm vertex distance.

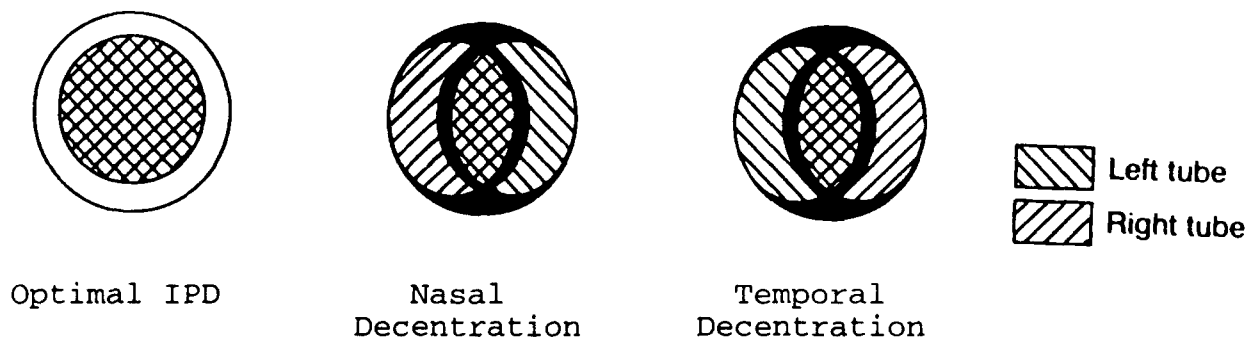
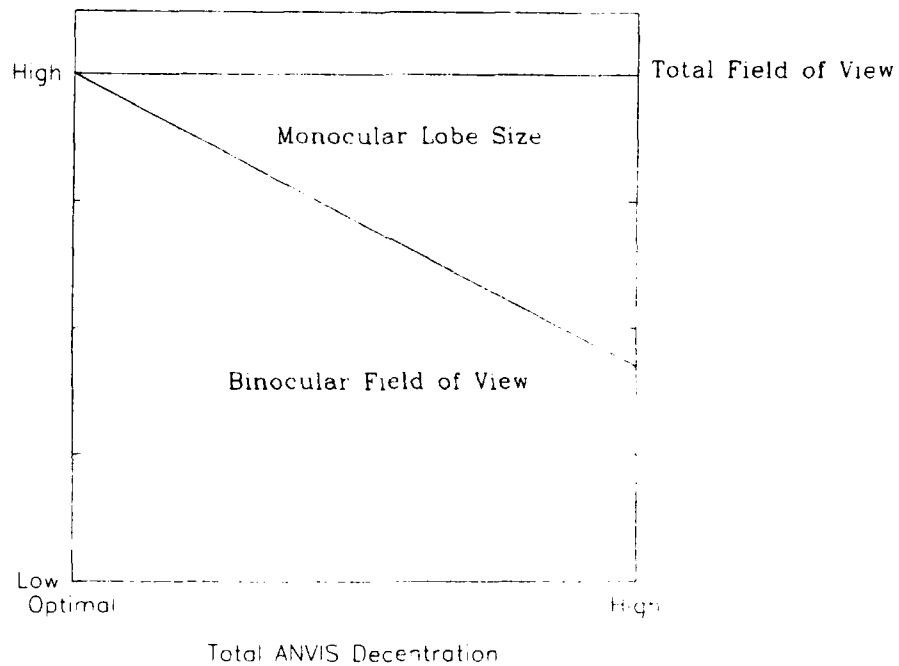
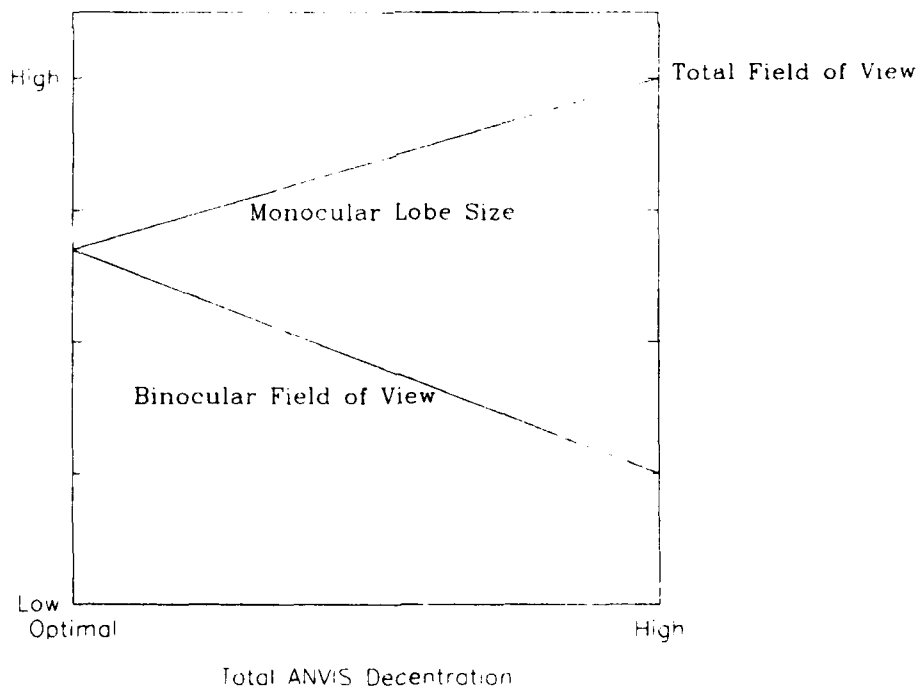


Figure 2. Predicted components of the field-of-view at 32 mm vertex distance.



**Figure 3. Relative contributions to the field-of-view at 18 mm vertex distance.**



**Figure 4. Relative contributions to the field-of-view at 32 mm vertex distance.**

Biberman and Alluisi (1992) have suggested that the performance of night vision devices is severely compromised by missetting the IPD. Hickok (1992) has reported that missetting ANVIS IPD by 10 mm can produce Snellen acuities of 20/200, or a logMAR score of 1.0. An extensive examination of the available data on this issue has led us to the belief that Hickok's data were probably based on unpublished studies of the AN/PVS-5A night vision goggle system conducted at USAARL in the early 1980's (McLean, 1992). However, there is clearly a need for a well documented investigation of the relationship between IPD setting and acuity in ANVIS.

The objectives of this research are to (1) verify the theoretical predictions described above with regard to the size of the components of the field-of-view as a function of changes in vertex distance and IPD in ANVIS, (2) document the impacts of changes in location in the field-of-view, vertex distance, and IPD on acuity in ANVIS, and (3) replicate earlier research on the impact of contrast on acuity with ANVIS.

### Methods

#### Subjects

Ten volunteer subjects participated in the field-of-view determinations. This group consisted of six males and four females, with an average age of  $30 \pm 10$  years. Eight volunteer subjects participated in the acuity determinations, four males and four females with an average age of  $28 \pm 8$  years. All subjects were able to achieve an 18 mm vertex distance and 20/45 acuity (logMAR = .35) on the high contrast Bailey-Lovie acuity chart, which is described below, through the ANVIS at the center of its field-of-view before the field-of-view session. Two subjects were unable to satisfy the acuity standard before the start of the acuity testing due to astigmatism, and were excluded from that portion of the experiment.

#### ANVIS

All measures were collected through a single flight certified set of ANVIS, which was used throughout the experiment. These ANVIS were attached to a customized mount and placed on an optical rail. A chin and forehead rest was also attached to the rail. This apparatus is shown in front and back quartering views in Figures 5 and 6. A black drape, not shown in the figure, was placed around the ANVIS tubes and over the mount to block stray light. The ANVIS, mounted to this rail, was positioned 10 feet from, and normal to, a black wall. Objective lens focusing and the tilt, vertical, IPD, and vertex distance adjustments were accomplished by the experimenters as outlined in Loro (1991). The subjects' IPDs were determined clinically using an IPD ruler.

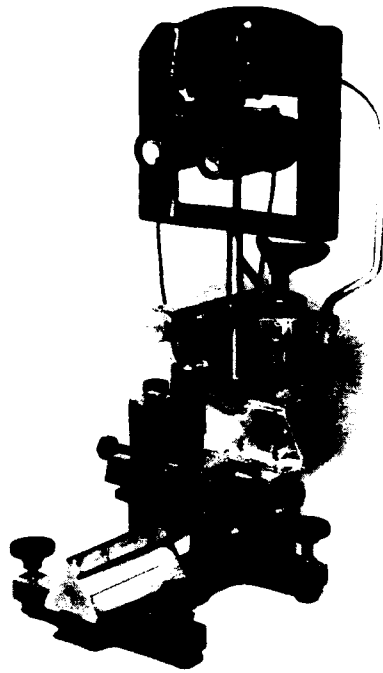


Figure 5. Front view of the apparatus.

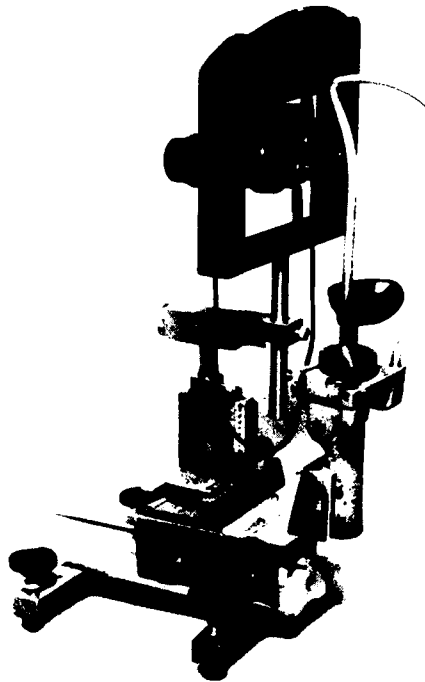


Figure 6. Rear view of the apparatus.

The 18 mm vertex distance position for the ANVIS was established using a House of Vision model 11 103 00 distometer (see Appendix A); the 32 mm vertex distance position was determined using the millimeter scale on the optical rail employed to position and stabilize the ANVIS and the chin/head rest. The subjects focused the diopter ring as outlined in Loro (1991) under the supervision of the experimenters. Eye movements were permitted. The ANVIS were used with Gentex polished-surface filters (see Appendix A) placed over the objective lenses. These filters attenuate incident radiant flux approximately 5 log units across the wavelengths to which ANVIS is sensitive (Rash and Martin, 1989). IPD settings were accomplished using an IPD mm ruler. IPD decentrations were analyzed as absolute deviations from the optimal IPD setting for that subject.

#### Field-of-view

An American Optical Project-O-Chart projector model 11082 with a Praboline slide model 11179 (see Appendix A) was used to project a circular spot of light 0.27 degrees in size onto a mat black wall. Under conditions of optimal IPD, horizontal limits to the fields-of-view were assessed by determining the point at which subjects reported that half of the spot remained visible. Kotulak (in preparation) employed a similar procedure to measure fields-of-view. Under both of the decentration conditions, the subjects were instructed that one edge of each field would appear clear, while the other would appear to be fuzzy. The "half the spot visible" criterion was to be used on the clear side, while on the fuzzy side, they were instructed to place the spot at the most extreme position at which they could detect it. Fields-of-view were determined for each tube of the ANVIS independently. The objective lens of the tube not in use was covered with an opaque cap. Two adjustments were applied to these field-of-view data in order to correct them to infinity. The first adjustment was to remove the IPD from the total and binocular field-of-view assessments, as the single tube fields which contribute to these measures are offset from each other by the amount of the IPD. The second involved adjusting the sizes of the monocular fields-of-view for the change in effective power of the objective lens due to the 10 foot working distance. This correction added 0.36 degrees to each field-of-view. Lighting was provided by the fluorescent room lighting at controlled reduced brightness. A two-way all within subjects (2 levels of vertex distance, 18 mm and 32 mm; 3 levels of IPD, 51 mm, optimal, and 72 mm) design was applied to the field-of-view measures. Greenhouse and Geisser (1958; 1959) corrections were calculated for these analyses. As no outcomes were altered, unadjusted F tests are reported. Regression analyses using the absolute amount of decentration to predict the sizes of the components of the field-of-view were also employed. Significance ( $p$  less than or equal to .05) is indicated by an asterix (\*) on the relevant figures. There were 28 degrees of freedom in these analyses. Absolute decentration

was chosen as an independent measure because theoretical analyses (Kotulak, 1992; McLean, 1992) indicated, and preliminary data analyses confirmed, that direction of decentration of IPD was irrelevant to the field-of-view measures.

### Acuity

Acuity measures were taken using Bailey-Lovie high (90%) contrast and low (8%) contrast visual acuity charts 4, 5, 6, and 7 (University of California, Berkeley, 1988; see Appendix A). These charts provide letters of equal legibility, with the same number of letters on each row, controlled letter and row spacing, and a logarithmic progression of letter size (Bailey and Lovie, 1976). The acuity data were collected and analyzed as logMAR scores. The scores were corrected for the difference in distance to the acuity targets between the center and the periphery of the field-of-view. Center field acuities were obtained with the acuity chart centered in the binocular portion of the field-of-view. Left and right limit acuities were measured with the acuity chart against the left or right limit of the overall visual field. For these conditions, the charts were placed so that, for the high contrast condition, the outermost character on the 0.5 logMAR line was placed as close to the edge as possible while still remaining readable. For the low contrast condition, this criterion was applied to the 0.8 logMAR line. Under conditions of decentration, these latter measures were expected to reflect monocular acuities, as well. Lighting was provided by (1) the fluorescent room lighting at controlled reduced brightness, and (2) two auxiliary dual tube 40 watt 48 inch fluorescent light fixtures. These two auxiliary lights were placed horizontally on stands 75 cm above the floor, 210 cm from and 40 cm below the acuity targets, and were separated from each other by 50 cm. They were set parallel to the wall. The reflectors on the auxiliary lamps shielded the ANVIS from their direct light. This arrangement provided luminances of 64.0, 71.9, and 59.6 candelas per meter squared on the Bailey-Lovie charts at the left, center, and right extremes of the fields-of-view employed in this experiment. These measurements were made with a Minolta nt-1 luminance meter (see Appendix A). This lighting arrangement was chosen because, during pilot experimentation, it yielded acuities in the range of those reported by Kotulak and Rash (1992) for quarter moon conditions using the Bailey-Lovie high and low contrast charts. A four-way all within subjects (2 levels of vertex distance, 18 mm and 32 mm; 3 levels of IPD, 51 mm, optimal, and 72 mm; 2 levels of location in the field-of-view, center and periphery; and 2 levels of contrast, high and low) design was applied to the acuity portion of this project. Greenhouse and Geisser (1958; 1959) corrections were calculated for this analysis. As no outcomes were altered, unadjusted F tests are reported. Regression analyses using relative decentration of IPD to predict acuity were also employed. Significance (p less than or equal to .05)

is indicated by an asterix (\*) on the relevant figures. There were 22 degrees of freedom in these analyses.

### Experimental sequence

The experimenters provided the subjects an initial briefing, during which the subjects were asked to give informed consent to participate in the experiment, and during which they were familiarized with the experimental procedure and the apparatus to be employed. The experimenters then measured the subject's IPD in order to determine the subject's optimal IPD. The experiment was divided into two sessions separated by a break. The first session was devoted to field-of-view measures, while the second consisted entirely of acuity measures. Each session required roughly 45 minutes to complete. The field-of-view session began with the subject focusing the ANVIS diopter ring. The experimenters then set the vertex distance to 18 mm and the optimal IPD. Monocular fields-of-view limits were determined for the left and right tubes independently. The IPD was reset to 72 mm for the second set of measures, and to 51 mm for the final set. The vertex distance was then adjusted to 32 mm, and the entire sequence was repeated. All subjects received this same sequence of conditions for the field-of-view determinations. The second, or acuity session, again began with the subject focusing the ANVIS diopter ring. The experimenters then set vertex distance to either 18 or 32 mm, and the IPD to either optimum, 72 mm, or 51 mm. In this session, 4 subjects experienced the 18 mm vertex conditions first, while 4 experienced the 32 mm vertex condition first. IPDs were presented in the same randomly determined order at both vertex distances for a particular subject. Overall, optimal IPD was presented first twice, second once, and third five times. The 72 mm IPD was presented first four times and second four times. The 51 mm IPD was presented first twice, second three times, and third three times. At each of these settings, acuity was measured in the center of the visual field, first under high and then under low contrast conditions, then at the left limit of the total field-of-view under high and low contrast conditions, and finally at the right limit of the total field-of-view under high and low contrast. Two variations of the Bailey-Lovie chart were used in this session. One was used for a set of high and low contrast measures, and the other was used for the next set of measures. The single alternation procedure was employed throughout the session. The experimenters then conducted an exit briefing, and dismissed the subject.

### Results

The average single tube field-of-view is the mean of the angular sizes of the left and right single tube fields-of-view. For the average single tube field-of-view size, there was a significant effect due to vertex distance ( $F(1,9) = 152.79$ ,  $p =$



.000001), IPD ( $F(2,18) = 10.69$ ,  $p = .0009$ ), and a significant vertex distance by IPD interaction ( $F(2,18) = 5.50$ ,  $p = .014$ ). The single tube field-of-view was reduced at 32 mm vertex distance and at other than optimal IPD. The interaction indicates that the differences in field-of-view between the 18 mm and 32 mm vertex distances are reduced at the 51 mm and 72 mm IPD settings compared to the optimal setting. These data are presented in graphical form in Figure 7. Regression analyses applied to these data are presented in Figure 8 for the 18 mm vertex distance condition and in Figure 9 for the 32 mm vertex distance condition. In both cases, the equations are significant, and accounted for substantial portions of the variance.

The binocular field-of-view is that angular area visible through both tubes simultaneously. For the binocular field-of-view measure, there was a significant effect due to vertex distance ( $F(1,9) = 135.81$ ,  $p = .000001$ ) and to IPD ( $F(2,18) = 13.07$ ,  $p = .0003$ ). The vertex distance by IPD interaction ( $F(2,18) = 0.69$ ,  $p = .52$ ) was not significant. The binocular field-of-view was greater at 18 mm vertex distance than at 32 mm vertex distance, and was greater at the optimal IPD setting than at the 51 mm or 72 mm settings for both vertex distances. These data are presented in graphical form in Figure 10. Regression analyses applied to these data are presented in Figure 11 for the 18 mm vertex distance condition and in Figure 12 for the 32 mm vertex distance condition. In both cases, the equations were significant, and accounted for substantial portions of the variance.

The monocular lobe size is the sum of the two lobes which represent the area visible to only one eye. For the monocular lobe size measure, there was a significant effect due to vertex distance ( $F(1,9) = 102.81$ ,  $p = .000003$ ), IPD ( $F(2,18) = 15.62$ ,  $p = .0001$ ), and a significant vertex distance by IPD interaction ( $F(2,18) = 9.22$ ,  $p = .002$ ). Monocular lobe size was smallest at optimal IPD settings and at 18 mm vertex distance. The interaction indicates that monocular lobe size increased more rapidly with increasing decentration at 32 mm vertex distance than at 18 mm vertex distance. These data are presented graphically in Figure 13. Regression analyses applied to these data are presented in Figure 14 for the 18 mm vertex distance and in Figure 15 for the 32 mm vertex distance. In both cases, the equations are significant, and accounted for substantial portions of the variance.

The total field-of-view extends from the left to the right edge of the area visible through either tube, and represents the total angular area visible through one or both tubes. It consists of the binocular field-of-view plus the monocular lobes. For the total field-of-view, there was a significant effect due to vertex distance ( $F(1,9) = 52.92$ ,  $p = .00005$ ), IPD ( $F(2,18) =$

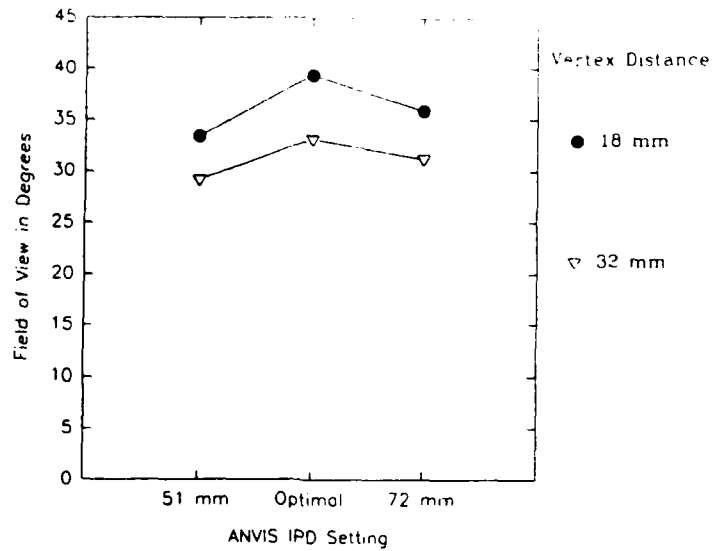


Figure 7. Average single tube field-of-view.

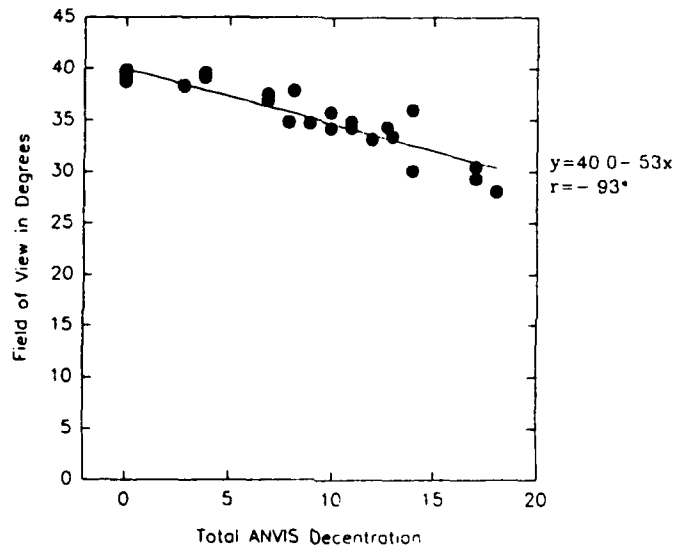


Figure 8. 18 mm vertex distance, average single tube field-of-view.

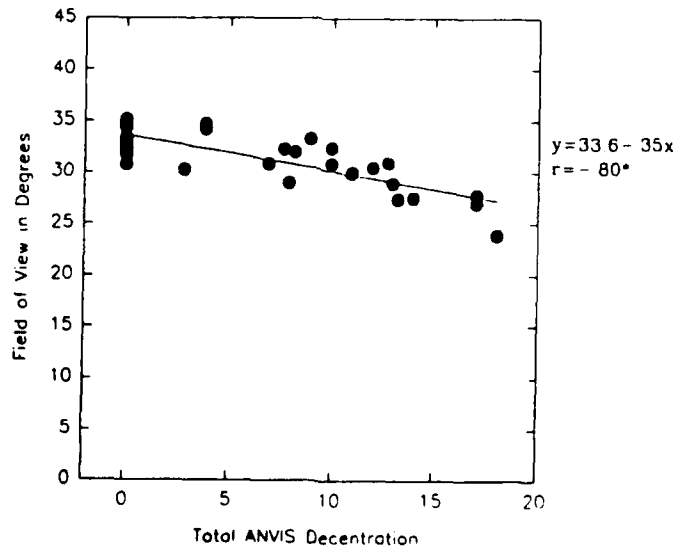


Figure 9. 32 mm vertex distance, average single tube field-of-view.

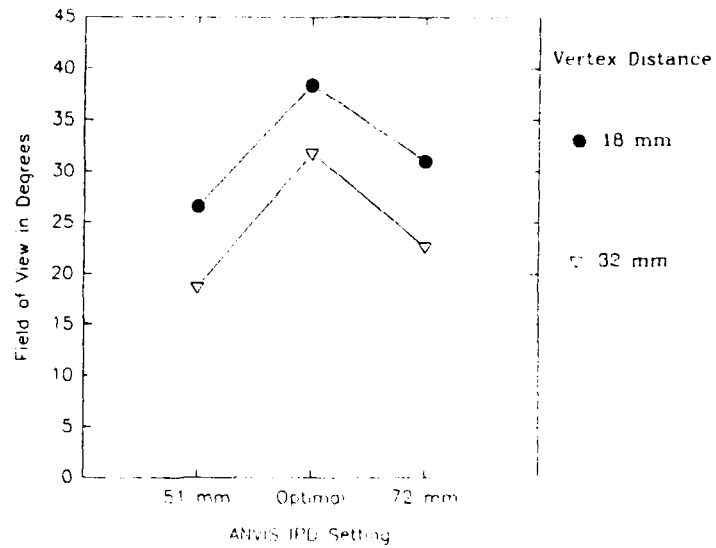


Figure 10. Binocular field-of-view.

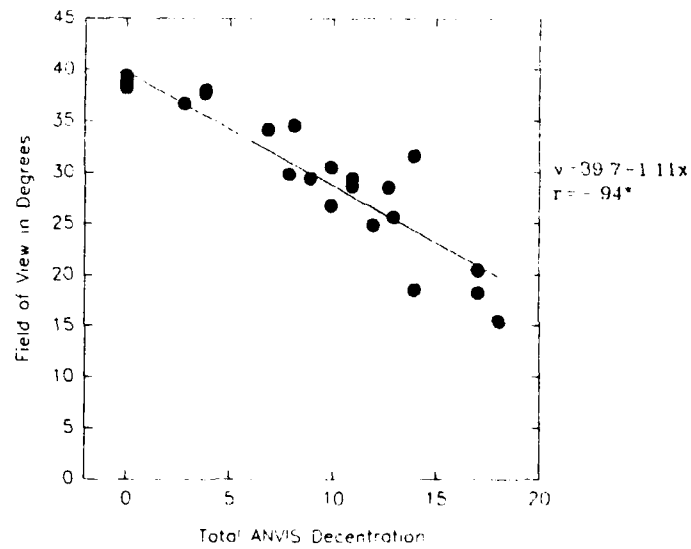


Figure 11. 18 mm vertex distance, binocular field-of-view.

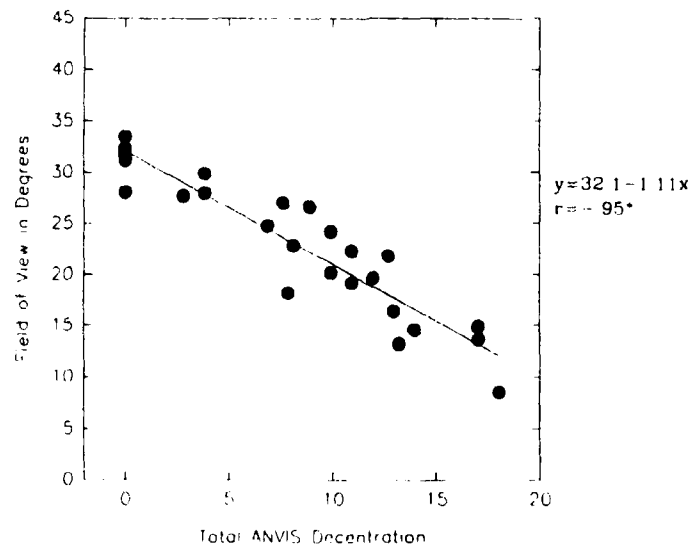


Figure 12. 32 mm vertex distance, binocular field-of-view.

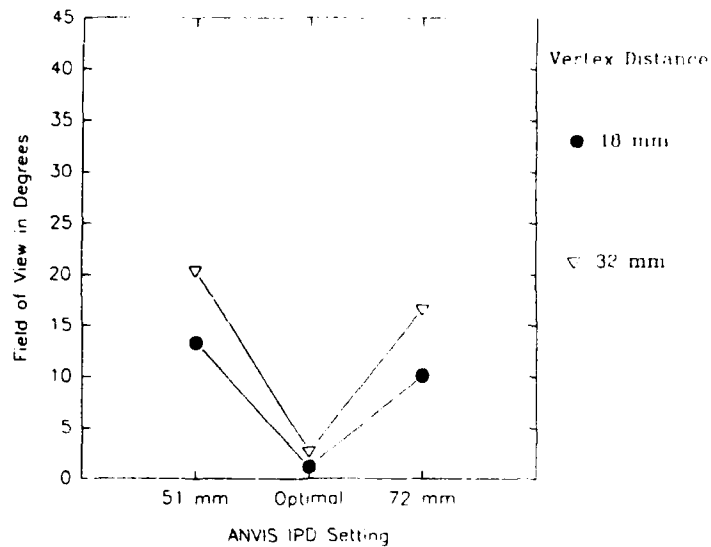


Figure 13. Monocular lobe size.

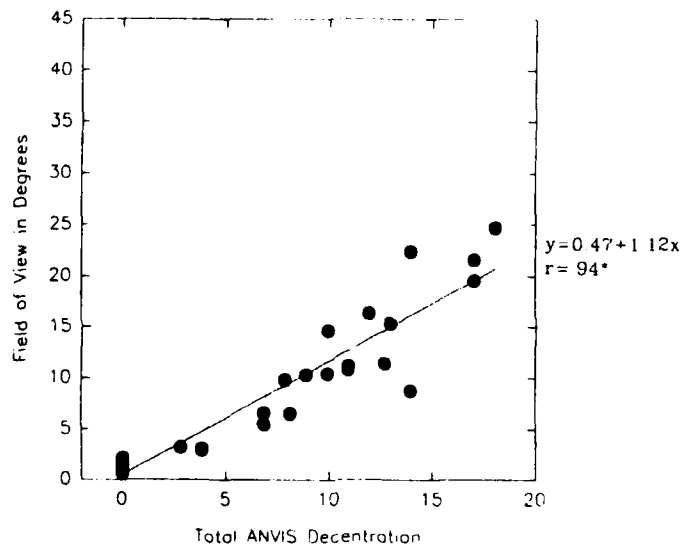


Figure 14. 18 mm vertex distance, monocular lobe size.

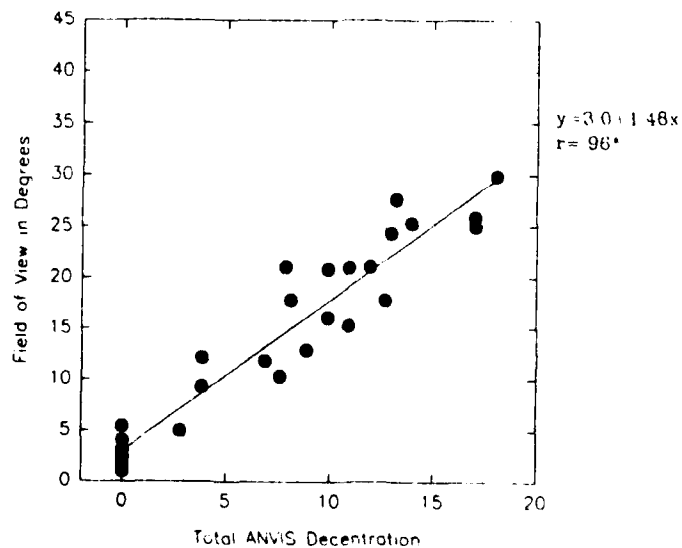


Figure 15. 32 mm vertex distance, monocular lobe size.

24.25,  $p = .000008$ ), and a significant vertex distance by IPD interaction ( $F(2,18) = 22.10$ ,  $p = .00001$ ). Total field-of-view was generally greater at 18 mm vertex distance than at 32 mm vertex distance, while the IPD effect and the IPD by vertex distance interaction reflect the convergence of 18 mm and 32 mm vertex distance total fields-of-view under conditions of decentration. These data are presented in graphical form in Figure 16. At 18 mm vertex distance, the total field-of-view was insensitive to decentration, but at 32 mm vertex distance, the total field-of-view increased with increasing decentration. While decentration appears to restore total field-of-view at 32 mm vertex distance, it should be noted that this applies only to the horizontal field-of-view. The field-of-view in the vertical meridian remains reduced in the face of increasing decentration. Regression analyses applied to these data are presented in Figure 17 for the 18 mm vertex distance condition and in Figure 18 for the 32 mm vertex distance condition. In the 32 mm vertex distance situation, the equation was significant, and accounted for a substantial portion of the variance.

The acuity data from the present experiment will be reported in logMARs. Table 1 contains conversions from logMARs to Snellen denominators. Analysis of the acuity data revealed that vertex distance had no effect on acuity ( $F(1,7) = 2.70$ ,  $p = .15$ ). IPD did influence acuity ( $F(2,14) = 4.57$ ,  $p = .03$ ), suggesting that acuity is slightly better at optimal IPD than it is under conditions of decentration. This effect indicates decreasing acuity with increasing decentration. Location in the visual field strongly influenced acuity ( $F(1,7) = 181.18$ ,  $p = .000003$ ), indicating that acuity was lower in the periphery than in the center of the visual field. Contrast also had a highly significant influence on acuity ( $F(1,7) = 1323.87$ ,  $p = .000000$ ), indicating greater acuity with high contrast than with low contrast stimuli. Location in the visual field interacted significantly with contrast ( $F(2,14) = 36.53$ ,  $p = .0005$ ), reflecting the reduced impact of low contrast in the periphery of the visual field compared to its center. The interactions of vertex distance and IPD ( $F(2,14) = 0.09$ ,  $p = .91$ ), vertex distance and location in the visual field ( $F(1,7) = 2.56$ ,  $p = .15$ ), IPD and location in the visual field ( $F(2,14) = 0.63$ ,  $p = .55$ ), vertex distance and contrast ( $F(1,7) = 0.005$ ,  $p = .95$ ), IPD and contrast ( $F(2,14) = 1.37$ ,  $p = .29$ ), vertex distance and IPD and location in the visual field ( $F(2,14) = 3.11$ ,  $p = .08$ ), vertex distance and IPD and contrast ( $F(2,14) = 0.16$ ,  $p = .86$ ), vertex distance and location in the visual field and contrast ( $F(1,7) = 5.32$ ,  $p = .055$ ), IPD and location in the visual field and contrast ( $F(2,14) = 0.71$ ,  $p = .51$ ), and the four-way interaction of vertex distance and IPD and location in the visual field and contrast ( $F(2,14) = 0.17$ ,  $p = .85$ ) did not achieve significance. These data are presented in Figure 19 for 18 mm vertex distance and in Figure 20 for 32 mm vertex distance.

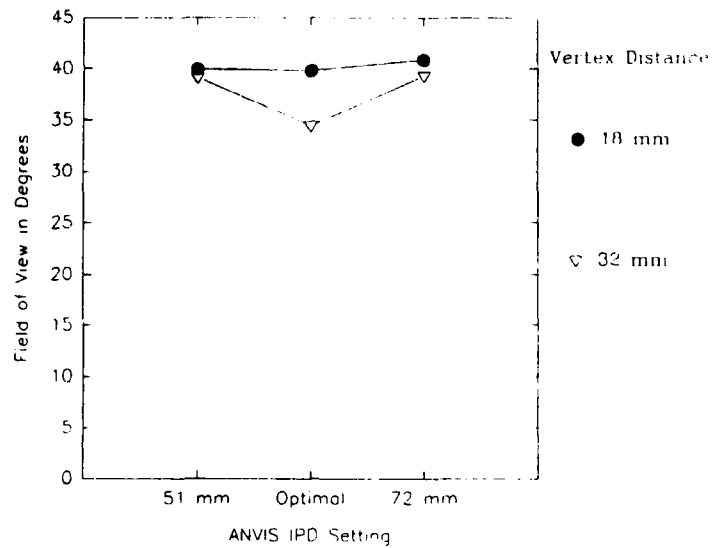


Figure 16. Total field-of-view.

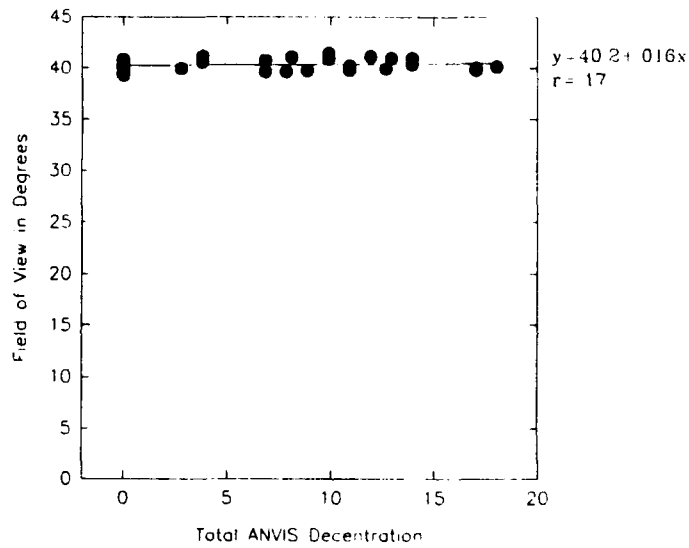


Figure 17. 18 mm vertex distance, total field-of-view.

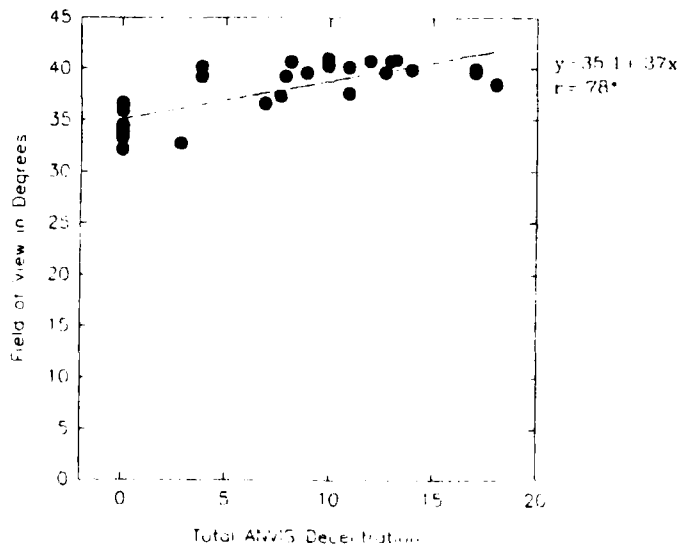


Figure 18. 32 mm vertex distance, total field-of-view.

Table 1.

Conversion from logMAR to Snellen Denominators (20/ - )

logMAR	Snellen Denominator
0	20.00
0.02	20.94
0.04	21.93
0.06	22.96
0.08	24.05
0.1	25.18
0.12	26.37
0.14	27.61
0.16	28.91
0.18	30.27
0.2	31.70
0.22	33.19
0.24	34.76
0.26	36.39
0.28	38.11
0.3	39.91
0.32	41.79
0.34	43.76
0.36	45.82
0.38	47.98
0.4	50.24
0.42	52.61
0.44	55.08
0.46	57.68
0.48	60.40
0.5	63.25
0.52	66.23
0.54	69.35
0.56	72.62
0.58	76.04
0.6	79.62
0.62	83.37
0.64	87.30
0.66	91.42
0.68	95.73
0.7	100.24
0.72	104.96
0.74	109.91
0.76	115.09
0.78	120.51
0.8	126.19
0.82	132.14
0.84	138.37
0.86	144.89
0.88	151.72
0.9	158.87
0.92	166.35
0.94	174.19
0.96	182.40
0.98	191.00
1	200.00

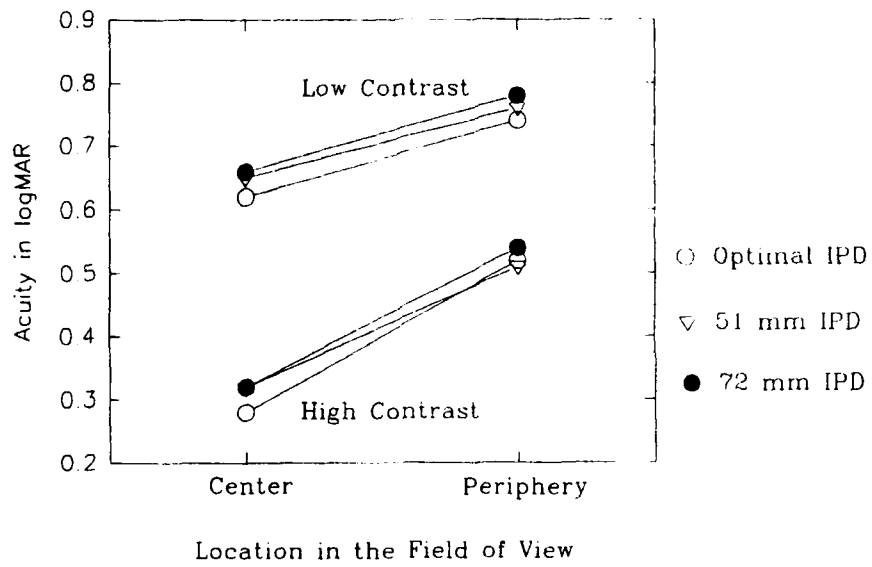


Figure 19. Acuity at 18 mm vertex distance.

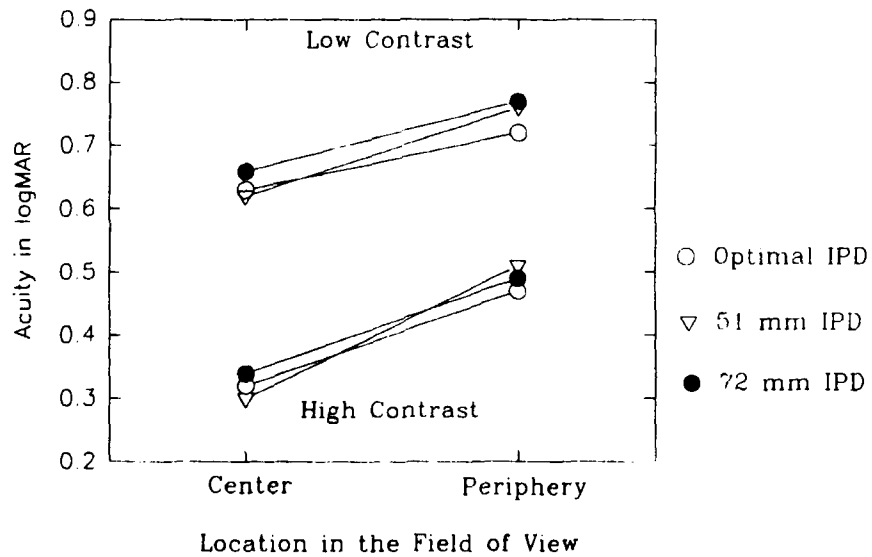


Figure 20. Acuity at 32 mm vertex distance.



Figures 21 through 24 present regression analyses employing decentration as the independent variable and acuity as the dependent variable under conditions of vertex distance, location in the field-of-view, and contrast employed in this experiment. Decentration was not a significant predictor of acuity in these regressions. The functions predict acuity changes of 1 letter or less on the Bailey-Lovie test charts for a decentration of 21 mm, the largest decentration possible with ANVIS.

### Discussion

#### Field-of-view

The single tube field-of-view results, which demonstrated a reduction in the size of the single tube field-of-view at 32 mm vertex distance compared to the 18 mm vertex distance, are consistent with the results obtained by other investigators (Kotulak, in preparation; Kotulak and Frezell, 1991; Walsh, unpublished, cited in Karney, 1988; Walsh, 1989; Walsh, 1990). These results are summarized and compared in Table 2. The low standard deviations speak well of our measurement technique.

Table 2.

Single tube fields-of-view in degrees as a function of vertex distance

Source	18 mm Vertex distance	32 mm Vertex distance
Walsh, 1989	39.8 $\pm$ .5	
Walsh, 1990, Figure 7	39.6	32.5
Walsh, unpublished, cited in Karney, 1988	39.5	
Kotulak, in preparation, Figure 8	39.8	33.4
This report	39.4 $\pm$ .3	33.1 $\pm$ 1.3

The decreases in single tube and binocular fields-of-view, and the increase in monocular lobe size seen at both 18 mm vertex distance and at 32 mm vertex distance with increasing decentration, as well as the increase in the size of the horizontal field-of-view at 32 mm vertex distance with increasing decentration are consistent with the theoretical analyses conducted by Kotulak (1992) and by McLean (1992). Our findings

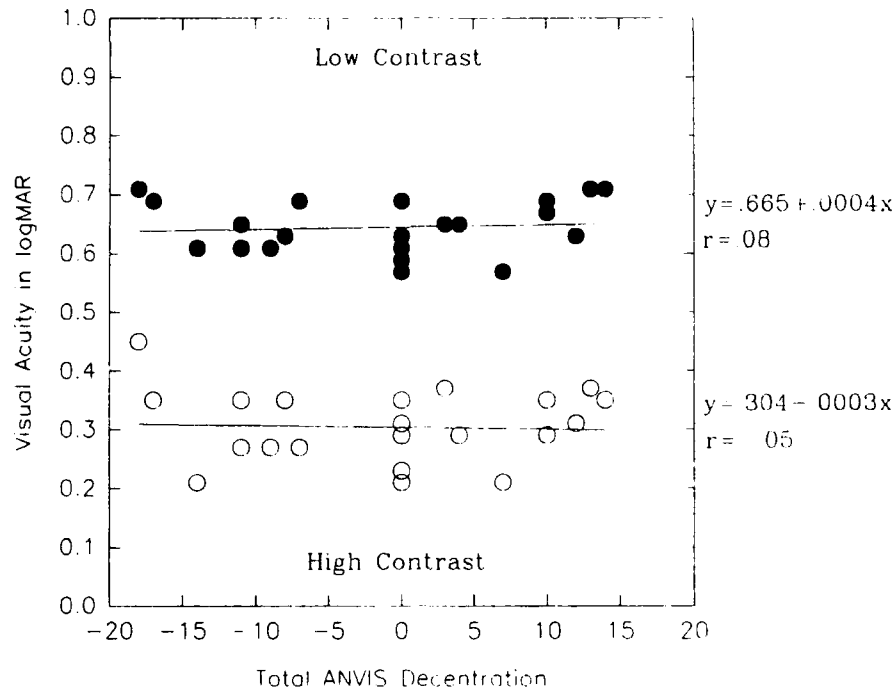


Figure 21. Acuity at 18 mm vertex distance, center of field.

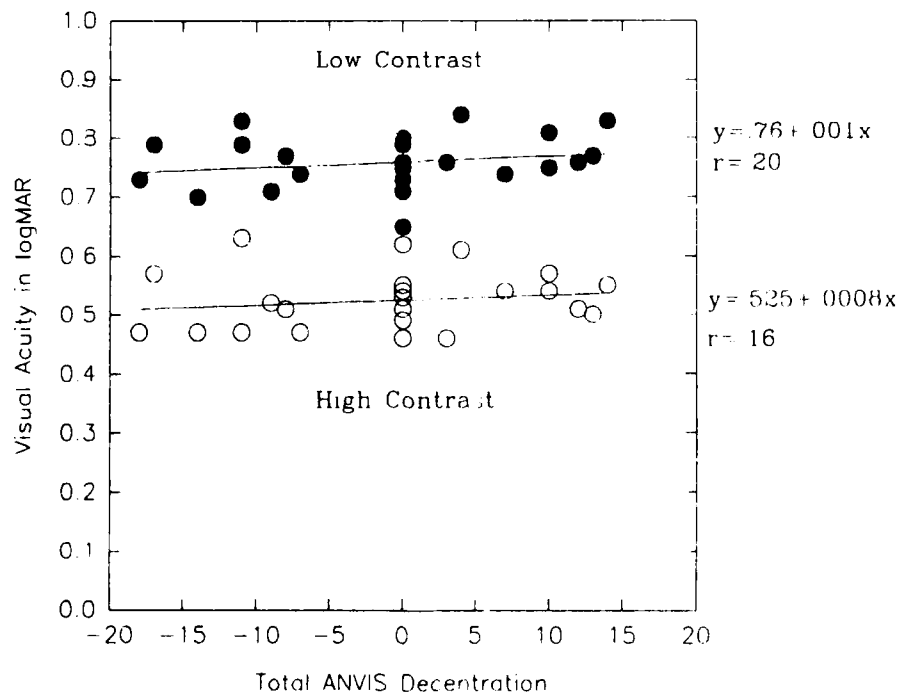


Figure 22. Acuity at 18 mm vertex distance, periphery of field.

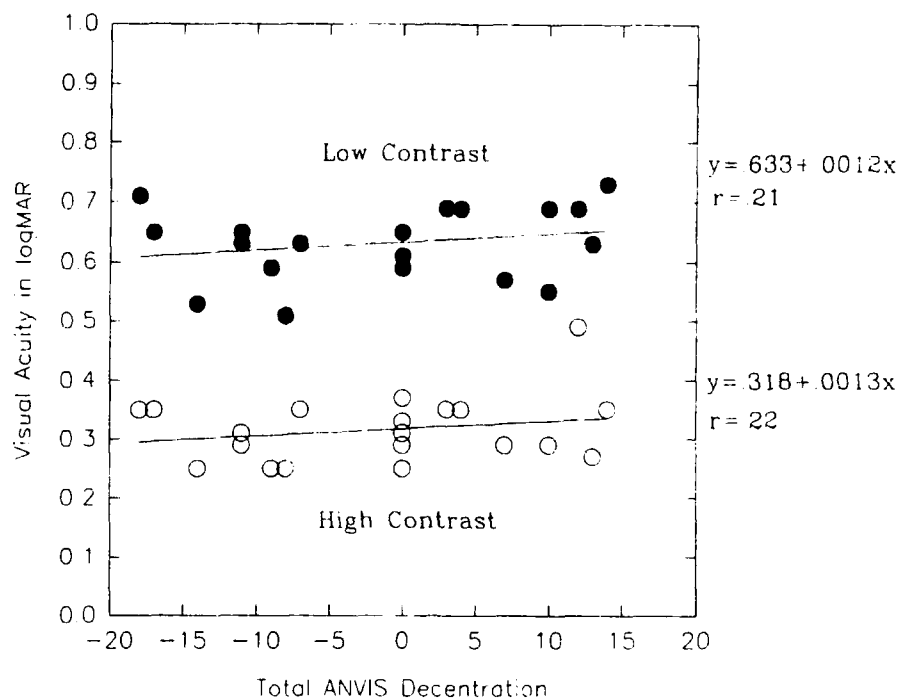


Figure 23. Acuity at 32 mm vertex distance, center of field.

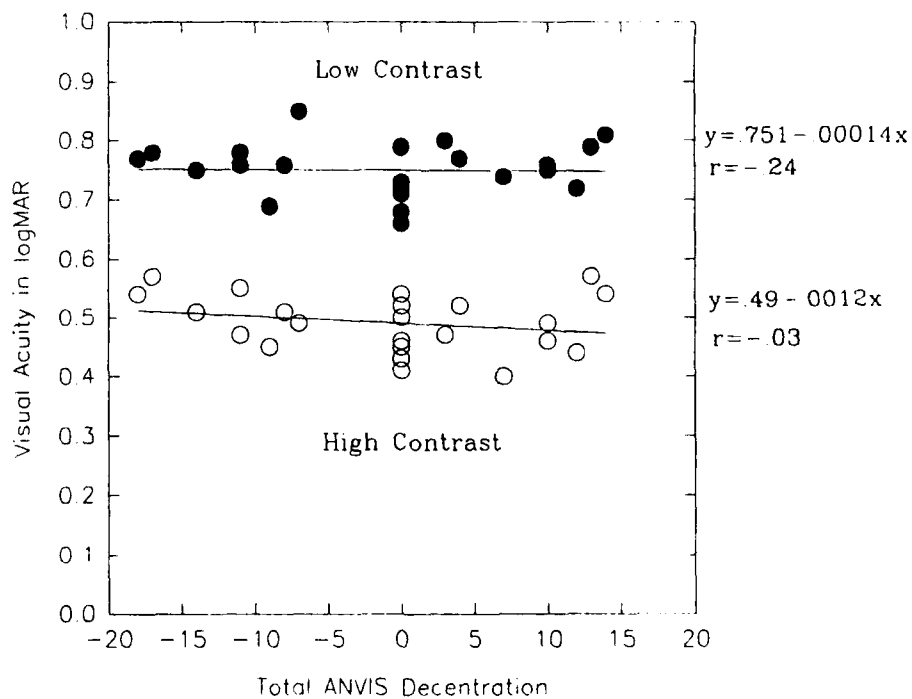


Figure 24. Acuity at 32 mm vertex distance, periphery of field.

in this regard are presented in Figure 25 for 18 mm vertex distance, summarizing Figures 11, 14, and 17, and in Figure 26 for 32 mm vertex distance, summarizing Figures 12, 15, and 18. The agreement with the theoretical analyses in Figures 3 and 4 is particularly striking. It should be noted that decentration does increase the total field-of-view at 32 mm vertex distance only for the horizontal total field-of-view. These analyses predict that the vertical field-of-view, which is also vignetted at 32 mm vertex distance, would remain reduced under decentration.

### Acuity

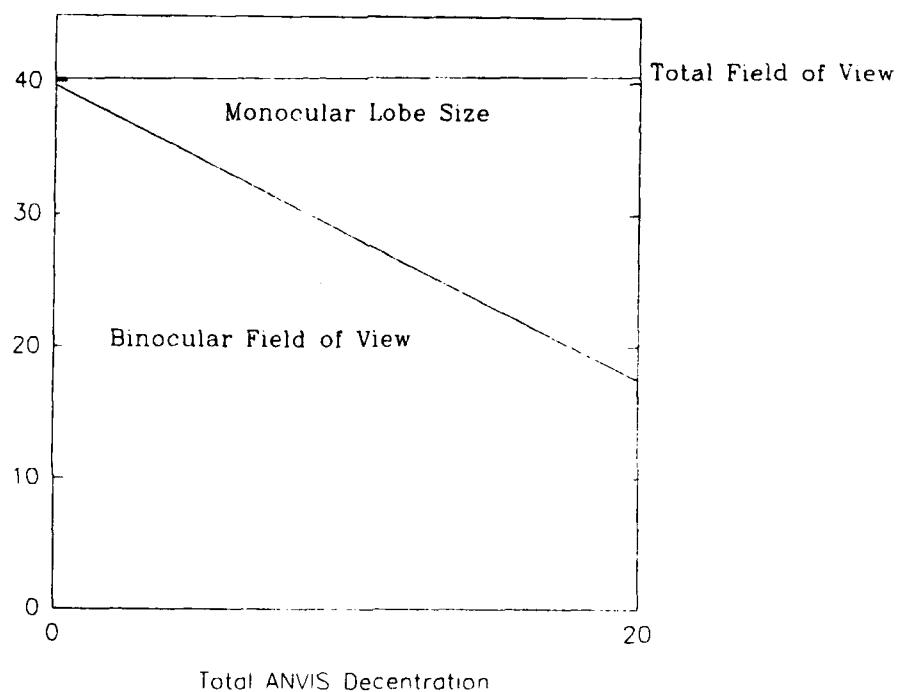
The acuity data obtained from the center and the periphery of the field-of-view were generally consistent with Walsh (unpublished, cited in Karney, 1988) except for the unusually low acuity he obtained under center field high contrast conditions. Indeed, our acuity data closely match Kotulak and Rash's (1992) results for the center of the field-of-view under both high and low contrast conditions. These data are summarized and compared in Table 3. The relative loss of acuity in the periphery of the ANVIS field-of-view is greater than previously reported.

Table 3.

Acuity in logMAR at the center and periphery of the ANVIS field-of-view for approximately equivalent lighting conditions

<u>Source</u>	<u>Center</u>	
	<u>High contrast</u>	<u>Low contrast</u>
Walsh unpublished, cited in Karney, 1988	.51 $\pm$ .08	.66 $\pm$ .04
Kotulak and Rash, 1992	.30 $\pm$ .08	.65 $\pm$ .15
This report	.28 $\pm$ .05	.62 $\pm$ .05
	<u>Periphery</u>	
	<u>High contrast</u>	<u>Low contrast</u>
Walsh, unpublished, cited in Karney, 1988	.58 $\pm$ .06	.73 $\pm$ .07
This report	.52 $\pm$ .05	.74 $\pm$ .05

Data are from Walsh's high luminance condition, Kotulak and Rash's quarter moon condition, and for the present report, the 18 mm vertex distance, optimal IPD condition.



**Figure 25. Observed relative contributions to the field-of-view at 18 mm vertex distance.**

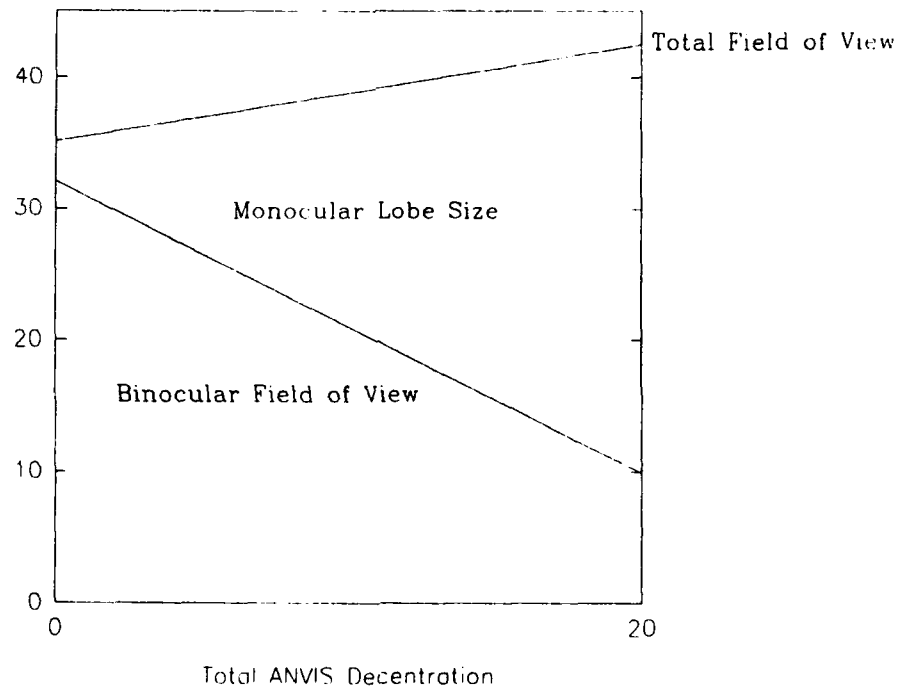


**Figure 26. Observed relative contributions to the field-of-view at 32 mm vertex distance.**

Although the effect of IPD was significant, it represents a small acuity loss, on average corresponding to one letter on the Bailey-Lovie charts under the most extreme decentration conditions. This is clearly not the severe deleterious effects on acuity which Hickok (1992) suggested should accompany even modest IPD decentration. Our results support the suggestion that Hickok's numbers are based on unpublished data from the AN/PVS-5 system, and do not represent results obtained from the later generation ANVIS (McLean, 1992). The present results reveal a statistically significant, but operationally inconsequential contribution of decentration to visual acuity, and do not support Biberman and Alluisi's (1992) contention that missetting the IPD will seriously reduce the performance of ANVIS.

The lack of an IPD by location in the visual field interaction in the present results indicates that the impact of peripheral versus central location in the field-of-view is the same under all conditions of decentration. This suggests that acuity is not reduced in the monocular lobes when compared to the binocular portions of the field-of-view. Examination of the angular sizes of the stimuli employed reveals that at the 10 foot working distance employed in the present experiments, the lines of Bailey-Lovie charts containing the thresholds had an angular size of 3.5 degrees for the high contrast stimuli and 5 degrees for the low contrast stimuli. Under conditions of IPD decentration, these critical lines were contained within the monocular lobe area in almost all cases in which peripheral acuities were being measured, while they were contained in the binocular portion of the field-of-view under optimal IPD conditions. On the other hand, these same lines were in the binocular field-of-view when central acuities were being measured, regardless of the decentration condition. These findings, consistent with Wiley's (1989) results comparing monocular and binocular systems, suggest that the monocular lobes have little impact on acuity with ANVIS.

Subjects in this experiment used the goggles under conditions of decentration for only relatively brief periods. Berkeley (1992) has suggested that decentration may have deleterious effects on visual performance over the course of a long mission. The present data do not address this issue, although it has been suggested that ANVIS and other night vision systems may produce visual fatigue (Brickner, 1989) and visual illusions (Crowley, 1991) under certain conditions. Indeed, several subjects commented on the unusual appearance of the visual field under conditions of moderate to high decentration. Further research into this question would be of value.

### Conclusions

At 18 mm vertex distance, binocular and monocular fields-of-view decreased with decentration of IPD setting, while monocular lobe size increased and the total field-of-view remained unchanged. At 32 mm vertex distance, binocular and monocular fields-of-view were reduced at optimal IPD, and decreased further with increasing decentration, while the monocular lobe size increased. At this vertex distance, the total horizontal field-of-view was restored to 40 degrees by modest decentration. Acuity was relatively insensitive to changes in vertex distance and IPD, but was substantially reduced in the periphery of the field-of-view and under conditions of low stimulus contrast.

## References

- Arditi, A. 1986. Binocular vision. in Boff, K.R., Kaufman, L., and Thomas, J.P. eds. Handbook of Perception and Human Performance. Volume 1, Sensory Processes and Perception. New York, NY: John Wiley and Sons, Inc. Chapter 23, 1-41.
- Bailey, I.L. and Lovie, J.E. 1976. New design principles for visual acuity letter charts. American Journal of Optometry and Physiological Optics. 53: 740-745.
- Berkeley, W.E. 1992. Williams Air Force Base, AZ: Armstrong Laboratory. Personal communication.
- Biberman, L.M. and Alluisi, E.A. 1992. Pilot Errors Involving Head-Up Displays (HUDs), Helmet-Mounted Displays (HMDs), and Night Vision Goggles (NVGs). Alexandria, VA: Institute for Defense Analyses. IDA Paper P-2638.
- Boff, K.R. and Lincoln, J.E. 1988. Engineering Data Compendium: Human Perception and Performance, Volume 1. Wright-Patterson Air Force Base, OH: AAMRL. 392-397.
- Brickner, M.S. 1989. Helicopter Flights with Night-Vision Goggles - Human Factors Aspects. Moffett Field, CA: Ames Research Center. Report No. N89-21477.
- Crowley, J.S. May 1991. Human Factors of Night Vision Devices: Anecdotes from the Field Concerning Visual Illusions and Other Effects. Fort Rucker, AL: U.S. Army Aeromedical Research Laboratory. USAARL Report No. 91-15.
- Greenhouse, S.W. and Geisser, S. 1958. Extension of Box's results on the use of the F distribution in multivariate analysis. Annals of Mathematical Statistics, 29, 95-112.
- Greenhouse, S.W. and Geisser, S. 1959. On methods in the analysis of profile data. Psychometrika, 24, 95-112.
- Hickok, S.M. 1992. Night vision goggle training in the United States Coast Guard. Aeromedical and Training Digest. (April) 1-3.
- Karney, D.H. 1988. Memorandum for Commander, CNVEO, Subject: Evaluation of the Aviator's Night Vision Imaging System (ANVIS) with 25mm Eyepieces. Fort Rucker, AL: U.S. Army Aeromedical Research Laboratory.
- Kotulak, J.C. 1992. Fort Rucker, AL: U.S. Army Aeromedical Research Laboratory. Personal communication.



- Kotulak, J.C. in preparation. Field-of-view Restrictions with the AN/AVS-6 Aviator Night Vision Imaging System. Fort Rucker, AL: U.S. Army Aeromedical Research Laboratory. USAARL Report.
- Kotulak, J.C. and Frezell, T.L. 1991. Field-of-View with night vision goggles. Paper presented at the 6th Annual Joint Services Night Vision Conference, 13 June, Phoenix, AZ.
- Kotulak, J.C. and Rash, C.E. 1992. Visual Acuity with Second and Third Generation Night Vision Goggles Obtained from a New Method of Night Sky Simulation Across a Wide Range of Target Contrast. Fort Rucker, AL: U.S. Army Aeromedical Laboratory. USAARL Report No. 92-9.
- Loro, S.L. 1991. NVG Operations. Fort Rucker, AL: U.S. Army Aviation Center.
- McLean, W.E. 1992. Fort Rucker, AL: U.S. Army Aeromedical Research Laboratory. Personal communication.
- Parry, R.B. 1992. Memorandum subject: Army Aviation Mishap Class A for OH-58D; Case Number 910816011. Fort Detrick, MD: U.S. Army Medical Research and Development Command.
- Rash, C.E. and Martin, J.S. 1989. ANVIS Lighting Compatibility Report: Auxiliary Lighting Program Flashlight Filters. Fort Rucker, AL: U.S. Army Aeromedical Research Laboratory. USAARL Letter Report No. 89-4-2-2.
- TC1-204. 1988. Night Flight Techniques and Procedures. Washington, DC: Headquarters, Department of the Army.
- University of California, Berkeley. 1988. Bailey-Lovie Distance Visual Acuity Charts. Berkeley, CA: University of California.
- U.S. Army Aviation Center. 1991. Exportable Training Package for NVG Operations. Fort Rucker, AL: U.S. Army Aviation Center. 902-011-T.
- Verona, R.W. and Rash, C.E. 1989. Human Factors and Safety Considerations of Night Vision Systems Flight. Fort Rucker, AL: U.S. Army Aeromedical Research Laboratory. USAARL Report No. 89-12.
- Walsh, D.J. 1989. Memorandum for Commander, Aviation Development Test Activity, Subject: ANVIS FOV measurement. Fort Rucker, AL: U.S. Army Aeromedical Research Laboratory.

- Walsh, D.J. February 1990. Laser Protection with Image Intensifier Night Vision Devices. Fort Rucker, AL: U.S. Army Aeromedical Research Laboratory. USAARL Report No. 90-3.
- Wells, M.J. and Venturino, M. 1989. The effects of increasing task complexity on the field-of-view requirements for a visually coupled system. Proceedings of the Human Factors Society 32nd Annual Meeting, Volume 2. Santa Monica, CA: Human Factors Society. 1429-1433.
- Wiley, R.W. 1989. Visual Acuity and Stereopsis with Night Vision Goggles. Fort Rucker, AL: U.S. Army Aeromedical Research Laboratory. USAARL Report No. 89-6.

Appendix A.

List of equipment manufacturers

American Optical Corporation  
Buffalo, NY 14215

Gentex Corporation  
Optical Products Group  
P.O. Box 315  
Carbondale, PA 18407

House of Vision Instrument Co.  
137 North Wabash Avenue  
Chicago, IL 60602

Minolta Corporation  
101 Williams Drive  
Ramsey, NJ 07446

University of California  
Multimedia Center  
School of Optometry  
Berkeley, CA 94270

Appendix B.

Data Collection Forms

Subject # \_\_\_\_\_ ANVIS # \_\_\_\_\_ Date \_\_\_\_\_

FOV

18mm VERTEX DISTANCE

----- Optimal IPD -----

Left FOV		Right FOV	
Left Limit	Right Limit	Left Limit	Right Limit
_____	_____	_____	_____

----- 72mm IPD -----

Left FOV		Right FOV	
Left Limit	Right Limit	Left Limit	Right Limit
_____	_____	_____	_____

----- 51mm IPD -----

Left FOV		Right FOV	
Left Limit	Right Limit	Left Limit	Right Limit
_____	_____	_____	_____

32mm VERTEX DISTANCE

----- Optimal IPD -----

Left FOV		Right FOV	
Left Limit	Right Limit	Left Limit	Right Limit
_____	_____	_____	_____

----- 72mm IPD -----

Left FOV		Right FOV	
Left Limit	Right Limit	Left Limit	Right Limit
_____	_____	_____	_____

----- 51mm IPD -----

Left FOV		Right FOV	
Left Limit	Right Limit	Left Limit	Right Limit
_____	_____	_____	_____

Subject # \_\_\_\_\_ ANVIS # \_\_\_\_\_ Date \_\_\_\_\_

Acuity

18mm VERTEX DISTANCE

Optimal IPD

Left		Center		Right	
High Con	Low Con	High Con	Low Con	High Con	Low Con
_____	_____	_____	_____	_____	_____

----- 72mm IPD -----

Left		Center		Right	
High Con	Low Con	High Con	Low Con	High Con	Low Con
_____	_____	_____	_____	_____	_____

----- 51mm IPD -----

Left		Center		Right	
High Con	Low Con	High Con	Low Con	High Con	Low Con
_____	_____	_____	_____	_____	_____

32mm VERTEX DISTANCE

----- Optimal IPD -----

Left		Center		Right	
High Con	Low Con	High Con	Low Con	High Con	Low Con
_____	_____	_____	_____	_____	_____

----- 72mm IPD -----

Left		Center		Right	
High Con	Low Con	High Con	Low Con	High Con	Low Con
_____	_____	_____	_____	_____	_____

----- 51mm IPD -----

Left		Center		Right	
High Con	Low Con	High Con	Low Con	High Con	Low Con
_____	_____	_____	_____	_____	_____

### Initial distribution

Commander, U.S. Army Natick Research,  
Development and Engineering Center  
ATTN: SATNC-MIL (Documents  
Librarian)  
Natick, MA 01760-5040

U.S. Army Communications-Electronics  
Command  
ATTN: AMSEL-RD-ESA-D  
Fort Monmouth, NJ 07703

Commander/Director  
U.S. Army Combat Surveillance  
and Target Acquisition Lab  
ATTN: DELCS-D  
Fort Monmouth, NJ 07703-5304

Commander  
10th Medical Laboratory  
ATTN: Audiologist  
APO New York 09180

Naval Air Development Center  
Technical Information Division  
Technical Support Detachment  
Warminster, PA 18974

Commanding Officer, Naval Medical  
Research and Development Command  
National Naval Medical Center  
Bethesda, MD 20814-5044

Deputy Director, Defense Research  
and Engineering  
ATTN: Military Assistant  
for Medical and Life Sciences  
Washington, DC 20301-3080

Commander, U.S. Army Research  
Institute of Environmental Medicine  
Natick, MA 01760

Library  
Naval Submarine Medical Research Lab  
Box 900, Naval Sub Base  
Groton, CT 06349-5900

Director, U.S. Army Human  
Engineering Laboratory  
ATTN: Technical Library  
Aberdeen Proving Ground, MD 21005

Commander  
Man-Machine Integration System  
Code 602  
Naval Air Development Center  
Warminster, PA 18974

Commander  
Naval Air Development Center  
ATTN: Code 602-B (Mr. Brindle)  
Warminster, PA 18974

Commanding Officer  
Armstrong Laboratory  
Wright-Patterson  
Air Force Base, OH 45433-6573

Director  
Army Audiology and Speech Center  
Walter Reed Army Medical Center  
Washington, DC 20307-5001

Commander, U.S. Army Institute  
of Dental Research  
ATTN: Jean A. Setterstrom, Ph. D.  
Walter Reed Army Medical Center  
Washington, DC 20307-5300

Naval Air Systems Command  
Technical Air Library 950D  
Room 278, Jefferson Plaza II  
Department of the Navy  
Washington, DC 20361

Commander, U.S. Army Test  
and Evaluation Command  
ATTN: AMSTE-AD-H  
Aberdeen Proving Ground, MD 21005

Director  
U.S. Army Ballistic  
Research Laboratory  
ATTN: DRXBR-OD-ST Tech Reports  
Aberdeen Proving Ground, MD 21005

Commander  
U.S. Army Medical Research  
Institute of Chemical Defense  
ATTN: SGRD-UV-AO  
Aberdeen Proving Ground,  
MD 21010-5425

Commander, U.S. Army Medical  
Research and Development Command  
ATTN: SGRD-RMS (Ms. Madigan)  
Fort Detrick, Frederick, MD 21702-5012

Director  
Walter Reed Army Institute of Research  
Washington, DC 20307-5100

HQ DA (DASG-PSP-O)  
5109 Leesburg Pike  
Falls Church, VA 22041-3258

Harry Diamond Laboratories  
ATTN: Technical Information Branch  
2800 Powder Mill Road  
Adelphi, MD 20783-1197

U.S. Army Materiel Systems  
Analysis Agency  
ATTN: AMXSY-PA (Reports Processing)  
Aberdeen Proving Ground  
MD 21005-5071

U.S. Army Ordnance Center  
and School Library  
Simpson Hall, Building 3071  
Aberdeen Proving Ground, MD 21005

U.S. Army Environmental  
Hygiene Agency  
Building E2100  
Aberdeen Proving Ground, MD 21010

Technical Library Chemical Research  
and Development Center  
Aberdeen Proving Ground, MD  
21010-5423

Commander  
U.S. Army Medical Research  
Institute of Infectious Disease  
SGRD-UIZ-C  
Fort Detrick, Frederick, MD 21702

Director, Biological  
Sciences Division  
Office of Naval Research  
600 North Quincy Street  
Arlington, VA 22217

Commander  
U.S. Army Materiel Command  
ATTN: AMCDE-XS  
5001 Eisenhower Avenue  
Alexandria, VA 22333

Commandant  
U.S. Army Aviation  
Logistics School ATTN: ATSQ-TDN  
Fort Eustis, VA 23604

Headquarters (ATMD)  
U.S. Army Training  
and Doctrine Command  
ATTN: ATBO-M  
Fort Monroe, VA 23651

Structures Laboratory Library  
USARTL-AVSCOM  
NASA Langley Research Center  
Mail Stop 266  
Hampton, VA 23665



Naval Aerospace Medical  
Institute Library  
Building 1953, Code 03L  
Pensacola, FL 32508-5600

Command Surgeon  
HQ USCENTCOM (CCSG)  
U.S. Central Command  
MacDill Air Force Base FL 33608

Air University Library  
(AUL/LSE)  
Maxwell Air Force Base, AL 36112

U.S. Air Force Institute  
of Technology (AFIT/LDEE)  
Building 640, Area B  
Wright-Patterson  
Air Force Base, OH 45433

Henry L. Taylor  
Director, Institute of Aviation  
University of Illinois-Willard Airport  
Savoy, IL 61874

Chief, Nation Guard Bureau  
ATTN: NGB-ARS (COL Urbauer)  
Room 410, Park Center 4  
4501 Ford Avenue  
Alexandria, VA 22302-1451

Commander  
U.S. Army Aviation Systems Command  
ATTN: SGRD-UAX-AL (LTC Gillette)  
4300 Goodfellow Blvd., Building 105  
St. Louis, MO 63120

U.S. Army Aviation Systems Command  
Library and Information Center Branch  
ATTN: AMSAV-DIL  
4300 Goodfellow Boulevard  
St. Louis, MO 63120

Federal Aviation Administration  
Civil Aeromedical Institute  
Library AAM-400A  
P.O. Box 25082  
Oklahoma City, OK 73125

Commander  
U.S. Army Academy  
of Health Sciences  
ATTN: Library  
Fort Sam Houston, TX 78234

Commander  
U.S. Army Institute of Surgical Research  
ATTN: SGRD-USM (Jan Duke)  
Fort Sam Houston, TX 78234-6200

AAMRL/HEX  
Wright-Patterson  
Air Force Base, OH 45433

John A. Dellinger,  
Southwest Research Institute  
P. O. Box 28510  
San Antonio, TX 78284

Product Manager  
Aviation Life Support Equipment  
ATTN: AMCPM-ALSE  
4300 Goodfellow Boulevard  
St. Louis, MO 63120-1798

Commander  
U.S. Army Aviation  
Systems Command  
ATTN: AMSAV-ED  
4300 Goodfellow Boulevard  
St. Louis, MO 63120

Commanding Officer  
Naval Biodynamics Laboratory  
P.O. Box 24907  
New Orleans, LA 70189-0407

Assistant Commandant  
U.S. Army Field Artillery School  
ATTN: Morris Swott Technical Library  
Fort Sill, OK 73503-0312

Commander  
U.S. Army Health Services Command  
ATTN: HSOP-SO  
Fort Sam Houston, TX 78234-6000

HQ USAF/SGPT  
Bolling Air Force Base, DC 20332-6188

U.S. Army Dugway Proving Ground  
Technical Library, Building 5330  
Dugway, UT 84022

U.S. Army Yuma Proving Ground  
Technical Library  
Yuma, AZ 85364

AFFTC Technical Library  
6510 TW/TSTL  
Edwards Air Force Base,  
CA 93523-5000

Commander  
Code 3431  
Naval Weapons Center  
China Lake, CA 93555

Aeromechanics Laboratory  
U.S. Army Research and Technical Labs  
Ames Research Center, M/S 215-1  
Moffett Field, CA 94035

Sixth U.S. Army  
ATTN: SMA  
Presidio of San Francisco, CA 94129

Commander  
U.S. Army Aeromedical Center  
Fort Rucker, AL 36362

U.S. Air Force School  
of Aerospace Medicine  
Strughold Aeromedical Library Technical  
Reports Section (TSKD)  
Brooks Air Force Base, TX 78235-5301

Dr. Diane Damos  
Department of Human Factors  
ISSM, USC  
Los Angeles, CA 90029-0021

U.S. Army White Sands  
Missile Range  
ATTN: STEWS-IM-ST  
White Sands Missile Range, NM 88002

U.S. Army Aviation Engineering  
Flight Activity  
ATTN: SAVTE-M (Tech Lib) Stop 217  
Edwards Air Force Base, CA 93523-5000

Ms. Sandra G. Hart  
Ames Research Center  
MS 262-3  
Moffett Field, CA 94035

Commander, Letterman Army Institute  
of Research  
ATTN: Medical Research Library  
Presidio of San Francisco, CA 94129

Commander  
U.S. Army Medical Materiel  
Development Activity  
Fort Detrick, Frederick, MD 21702-5009

Commander  
U.S. Army Aviation Center  
Directorate of Combat Developments  
Building 507  
Fort Rucker, AL 36362

U. S. Army Research Institute  
Aviation R&D Activity  
ATTN: PERI-IR  
Fort Rucker, AL 36362

Commander  
U.S. Army Safety Center  
Fort Rucker, AL 36362

U.S. Army Aircraft Development  
Test Activity  
ATTN: STEBG-MP-P  
Cairns Army Air Field  
Fort Rucker, AL 36362

Commander U.S. Army Medical Research  
and Development Command  
ATTN: SGRD-PLC (COL Schnakenberg)  
Fort Detrick, Frederick, MD 21702

MAJ John Wilson  
TRADOC Aviation LO  
Embassy of the United States  
APO New York 09777

Netherlands Army Liaison Office  
Building 602  
Fort Rucker, AL 36362

British Army Liaison Office  
Building 602  
Fort Rucker, AL 36362

Italian Army Liaison Office  
Building 602  
Fort Rucker, AL 36362

Directorate of Training Development  
Building 502  
Fort Rucker, AL 36362

Chief  
USAHEL/USAAVNC Field Office  
P. O. Box 716  
Fort Rucker, AL 36362-5349

Commander U.S. Army Aviation Center  
and Fort Rucker  
ATTN: ATZQ-CG  
Fort Rucker, AL 36362

Chief  
Test & Evaluation Coordinating Board  
Cairns Army Air Field  
Fort Rucker, AL 36362

MAJ Terry Newman  
Canadian Army Liaison Office  
Building 602  
Fort Rucker, AL 36362

German Army Liaison Office  
Building 602  
Fort Rucker, AL 36362

LTC Patrice Cottebrune  
French Army Liaison Office  
USAAVNC (Building 602)  
Fort Rucker, AL 36362-5021

Australian Army Liaison Office  
Building 602  
Fort Rucker, AL 36362

Dr. Garrison Rapmund  
6 Burning Tree Court  
Bethesda, MD 20817

Commandant, Royal Air Force  
Institute of Aviation Medicine  
Farnborough Hampshire GU14 6SZ UK

Commander  
U.S. Army Biomedical Research  
and Development Laboratory  
ATTN: SGRD-UBZ-I  
Fort Detrick, Frederick, MD 21702

Defense Technical Information  
Cameron Station, Building 5  
Alexandra, VA 22304-6145

Commander, U.S. Army Foreign Science  
and Technology Center  
AIFRTA (Davis)  
220 7th Street, NE  
Charlottesville, VA 22901-5396

Director,  
Applied Technology Laboratory  
USARTL-AVSCOM  
ATTN: Library, Building 401  
Fort Eustis, VA 23604

U.S. Air Force Armament  
Development and Test Center  
Eglin Air Force Base, FL 32542

Commander, U.S. Army Missile  
Command  
Redstone Scientific Information Center  
ATTN: AMSMI-RD-CS-R  
/ILL Documents  
Redstone Arsenal, AL 35898

Dr. H. Dix Christensen  
Bio-Medical Science Building, Room 753  
Post Office Box 26901  
Oklahoma City, OK 73190

Director  
Army Personnel Research Establishment  
Farnborough, Hants GU14 6SZ UK

U.S. Army Research and Technology  
Laboratories (AVSCOM)  
Propulsion Laboratory MS 302-2  
NASA Lewis Research Center  
Cleveland, OH 44135

Dr. Christine Schlichting  
Behavioral Sciences Department  
Box 900, NAVUBASE NLON  
Groton, CT 06349-5900

Dr. Eugene S. Channing  
7985 Schooner Court  
Frederick, MD 21701-3273

LTC Gaylord Lindsey (5)  
USAMRDC Liaison at Academy  
of Health Sciences  
ATTN: HSHA-ZAC-F  
Fort Sam Houston, TX 78234

Aviation Medicine Clinic  
TMC #22, SAAF  
Fort Bragg, NC 28305

Dr. A. Kornfield, President  
Biosearch Company  
3016 Revere Road  
Drexel Hill, PA 29026

NVEOD  
AMSEL-RD-ASID  
(Attn: Trang Bui)  
Fort Belvoir, VA 22060

CA Av Med  
HQ DAAC  
Middle Wallop  
Stockbridge Hants S020 8DY UK

Commander and Director  
USAE Waterways Experiment Station  
ATTN: CEWES-IM-MI-R  
Alfrieda S. Clark, CD Dept.  
3909 Halls Ferry Road  
Vicksburg, MS 39180-6199

Mr. Richard Thornley  
ILS Manager, APACHE  
Box 84  
Westland Helicopters Limited  
Yeovil, Somerset BA202YB UK

Col. Otto Schramm Filho  
c/o Brazilian Army Commission  
Office-CEBW  
4632 Wisconsin Avenue NW  
Washington, DC 20016